Pure appl. geophys. 162 (2005) 2111–2132
0033-4553/05/112111-22
DOI 10.1007/s00024-005-2710-y

Pure and Applied Geophysics

Volcanic Tremor at Mt. Etna, Italy, Preceding and Accompanying the Eruption of July – August, 2001

S. Falsaperla,[1] S. Alparone,[1] S. D'Amico,[1] G. Grazia,[1] F. Ferrari,[1] H. Langer,[1] T. Sgroi,[1] and S. Spampinato[1]

Abstract— The July 17 – August 9, 2001 flank eruption of Mt. Etna was preceded and accompanied by remarkable changes in volcanic tremor. Based on the records of stations belonging to the permanent seismic network deployed on the volcano, we analyze amplitude and frequency content of the seismic signal. We find considerable changes in the volcanic tremor which mark the transition to different styles of eruptive activity, e.g., lava fountains, phreatomagmatic activity, Strombolian explosions. In particular, the frequency content of the signal decreases from 5 Hz to 3 Hz at our reference station ETF during episodes of lava fountains, and further decreases at about 2 Hz throughout phases of intense lava emission. The frequency content and the ratios of the signal amplitude allow us to distinguish three seismic sources, i.e., the peripheral dike which fed the eruption, the reservoir which fed the lava fountains, and the central conduit. Based on the analysis of the amplitude decay of the signal, we highlight the migration of the dike from a depth of ca. 5 km to about 1 km between July 10 and 12. After the onset of the effusive phase, the distribution of the amplitude decay at our stations can be interpreted as the overall result of sources located within the first half kilometer from the surface. Although on a qualitative basis, our findings shed some light on the complex feeding system of Mt. Etna, and integrate other volcanological and geophysical studies which tackle the problem of magma replenishment for the July–August, 2001 flank eruption. We conclude that volcanic tremor is fundamental in monitoring Mt. Etna, not only as a marker of the different sources which act within the volcano edifice, but also of the diverse styles of eruptive activity.

Key words: Etna, volcanic tremor, eruption, seismicity.

Introduction

Mt. Etna is a basaltic stratovolcano with persistent volcanic activity situated in eastern Sicily, Italy. With its 3350 m of altitude above sea level (asl), it is the highest volcano in the Mediterranean region and one of the best monitored volcanic areas worldwide. Apart from continuous degassing, Mt. Etna's eruptions are mostly characterized by lava effusions, Strombolian activity, and spectacular lava fountains. We distinguish between summit and flank eruptions, depending on whether volcanic

[1]Istituto Nazionale di Geofisica e Vulcanologia, Sezione di Catania, P.zza Roma 2, 95123, Catania, Italy.

activity takes place at the summit craters or from the opening of lateral, eruptive fissures.

One of the most important flank eruptions of Mt. Etna in the past century occurred in the Valle del Bove (Fig. 1) between December 14, 1991 and March 31, 1993. The volcano erupted 235×10^6 m^3 of magma, forming a lava field with extension over 7.6 km^2 (e.g., BARBERI *et al.*, 1993; ARMIENTI *et al.*, 1994; CALVARI *et al.*, 1994). Prevalent degassing activity followed the 1991–1993 flank eruption, until a stage of short-lived summit lava emissions, overflows, and lava fountains started in 1995. In particular, from May 2001 there were fifteen episodes of lava fountains preceding the impending flank eruption. By July 13, 2001, a N-S striking field of fissures opened south of the SE crater, heralding the lava emission in the upper part of the Valle del Bove (Fig. 1). The volcano unrest started on July 17. Only some of the fissures, which continued to open throughout the flank eruption, yielded lava flows. Three main eruptive centers formed at altitudes between 2100 m and 3000 m asl (Fig. 1). From July 31 the rate of lava emission dropped rapidly, and on August 9, the eruption stopped completely. Eventually, the lava fronts reached their lowest elevation at 1035 m asl, a few kilometers away from the village of Nicolosi. Totally, 48×10^6 m^3 of lava were emitted with an estimated eruption rate of ca. 24 m^3 s^{-1}(Research staff of INGV, 2001). Throughout its 23 days of duration, the flank eruption evolved through different states of activity, during which the lava emission was temporary accompanied by powerful Strombolian explosions and phreatomagmatic activity (Research staff of INGV, 2001). Thick ash clouds formed during the paroxysmal phases, and the consequent fallout heavily affected the Etnean region according to the wind direction (Fig. 2). The ejected fine particles represented a potential hazard not only for health, but also for agriculture and traffic. Particularly the aerial transportation faced considerable damage for the repetitive closure of the airport of Catania Fontanarossa.

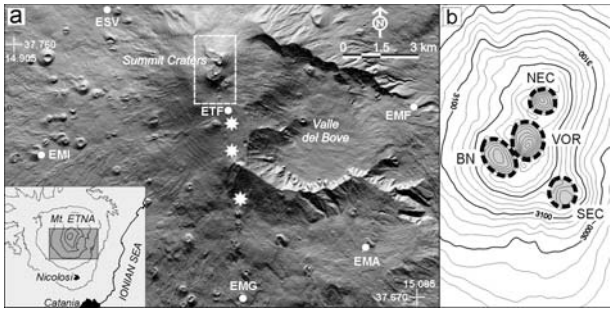

Figure 1

a) Map of Mt. Etna and location of the seismic stations considered in this study (full white circles). The inset (dashed white square) and the stars mark the location of the summit craters (enlarged in b) and the three main eruptive vents during the 2001 eruption, respectively. b) Location of the summit craters: Northeast Crater (NEC), Voragine (VOR), Southeast Crater (SEC), and Bocca Nuova (BN).

The continuous monitoring of seismic activity at Mt. Etna started in the late 1970s, and has allowed the identification of a variety of signals (e.g., PATANÈ *et al.*, 2004) such as: volcano tectonic (VT) earthquakes, long-period events, hybrid events, explosion quakes, and volcanic tremor. The flank eruption of July 17 – August 9, 2001 was preceded by an earthquake swarm which started in the late evening of July 12. VT seismicity also accompanied and followed the lava emission until July 18, reaching a total of 2645 events with magnitude $M_D \geq 1$ (Research staff of INGV, 2001). According to the hypocentral locations, the seismogenic zones were identified below the summit craters, up to a depth of 5 km below sea level (bsl) (PATANÈ *et al.*, 2003a). Following a seismic style reported during previous eruptive periods as well (e.g., CARDACI *et al.*, 1993; FALSAPERLA *et al.*, 1994, 2002), the VT earthquakes mostly faded a few days after the onset of the lava emission. Thus, we focused our attention on those seismic signals likely suggestive of the on-going eruptive dynamics also in the absence of VT seismicity. Particularly, in this paper we deal with volcanic tremor analysis, as changes in amplitude and frequency content of this signal preceded, accompanied, and marked the end of the flank eruption.

The importance of volcanic tremor in the seismic monitoring of Mt. Etna was put forward by SCHICK and RIUSCETTI (1973), who were the first to postulate a strict link between this signal and the volcano feeder. SCHICK *et al.* (1982), SEIDL *et al.* (1981),

Figure 2
Aerial view of Mt. Etna from northwest during the July – August, 2001 eruption. Vigorous emission of vapor and ejecta – moving in the direction of the trade winds – is visible well above the craters, which are located at about 3300 m altitude (courtesy of Mr. Alfio Amantia, INGV- Sez. Catania).

COSENTINO *et al.* (1989) used amplitude and spectral features of tremor for modeling the feeder to explore the complex volcanic structure.

A peculiar aspect of volcanic tremor at Mt. Etna is its continuity in time. This characteristic is not found in andesitie volcanoes such as Merapi, Indonesia, or Soufrière Hills, Montserrat, where tremor is recorded as a transient signal (e.g., SEIDL *et al.*, 1990; NEUBERG *et al.*, 1998); conversely, it is a feature common to other basaltic volcanoes with persistent activity like Stromboli, Italy, where such a continuity offers the opportunity to explore the relationship between tremor and volcanic activity (e.g., LANGER and FALSAPERLA, 2003).

Tremor is commonly addressed to as RMS amplitude of the seismic signal measured over a certain time window and frequency band (e.g., STEPHEN *et al.*, 1994; GORDEEV *et al.*, 1990; FALSAPERLA *et al.*, 1998). In this note, we focus our attention on the seismic radiation in the time and frequency domains from July to August, 2001. We analyze the development of the signal in time looking at the ratio of the RMS amplitude at different stations, and reconstruct the short-term evolution of volcanic tremor with reference to the main features of volcanic activity. Finally, we highlight the temporal links between the changes in volcanic tremor and the eruptive styles reported by volcanologists during the flank eruption.

Data Acquisition and Amplitude Analysis

The *Istituto Nazionale di Geofisica e Vulcanologia (INGV) - Sezione di Catania* runs a permanent seismic network on Mt. Etna, deployed at an altitude approximately ranging from 200 m to 2900 m. In the present work we use the data of six stations located at distances less than 10 km from the summit craters (Fig. 1). The reasons for our choice of these stations were twofold. First, we selected the stations which provided the longest data continuity during the period preceding and accompanying the July-August, 2001 flank eruption. Secondly, we considered the stations with the best signal to noise ratio, in order to analyze the characteristics of tremor not only during the paroxysms, but also throughout relatively quiet stages. In particular, we use ETF (Fig. 1) as a reference station for our analyses, as it is located near the field of fissures from which the lava emission began.

The stations are equipped with short-period (1 s) seismometers. The signals are radio transmitted to the data acquisition center in Catania, where they are digitized by a 12-bit A/D converter with a sampling rate of 160 Hz, and stored on a PC-based acquisition system. We process the seismic signals with a specific software which was developed by two of us (G. Di Grazia and F. Ferrari), computing the RMS amplitude at each station over a 30 s time window. In Figure 3 we depict the RMS amplitude at ETF from July 3 to August 13, 2001. In the cartoon, we marked off the earthquake swarm preceding and accompanying the unrest, as well as two styles of volcanic activity, i.e., lava fountains and the lava effusion. The RMS amplitude

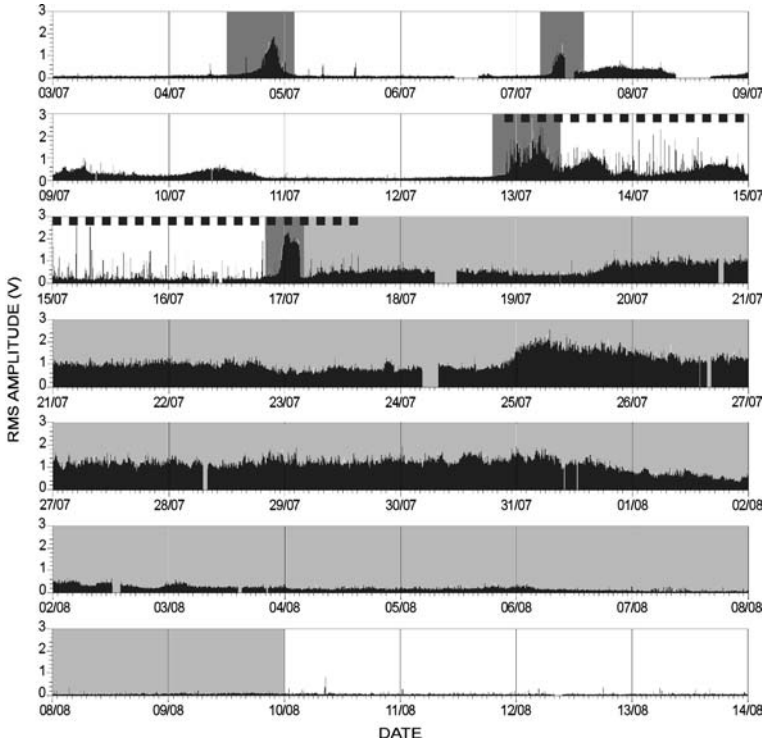

Figure 3
RMS tremor amplitude at ETF from July 3 to August 13, 2001. The different styles of volcanic activity are highlighted using a gray scale. White, lighter gray, and darker gray mark low volcanic activity, effusive period, and lava fountains, respectively. The dashed line marks the earthquake swarm preceding and accompanying the volcanic unrest. Short interruptions on the acquisition system produced gaps in the cartoon.

fluctuated until the seismic swarm began on July 12. Particularly, the large, temporary increments on July 4 and 7 were associated with two episodes of lava fountains. The start of the earthquake swarm and the lava fountain during the night of July 12 were associated with the transition to high RMS amplitude values (Fig. 3). Afterwards, the energy content of the seismic radiation remained high, with a climax on July 25. By July 31, the RMS amplitude decreased, marking the slow return to the background values.

In Table 1 we list 17 paroxysmal episodes — two episodes of powerful Strombolian activity and 15 lava fountains — preceding the volcanic unrest, and indicate their duration based on their corresponding seismic record. The start of each episode was fixed according to an empirical estimate when an amplitude threshold — defined as the mean amplitude value of the seismic signal at ETF — was overcome. The end of each episode was associated with the return to the background amplitude.

Table 1

Episodes of lava fountains and powerful Strombolian activity (marked with a star) from May 2001, and their duration based on seismic records

Start (in U.T.)	Duration (hours)
* May 07 05:15	15.75
* May 09 08:20	10.25
June 06 20:50	13.83
June 08 21:55	7.17
June 10 21:50	7.08
June 12 15:40	12.75
June 15 07:40	6.75
June 17 07:45	10.75
June 19 17:45	6.42
June 22 14:45	4.67
June 24 07:45	16.17
June 27 07:50	24.58
June 30 04:10	10.67
July 04 10:40	15.50
July 07 05:00	8.67
July 12 19:20	13.33
July 16 19:50	7.83

Spectral Analysis

Several studies focus on volcanic tremor for monitoring purposes. On Stromboli volcano, for instance, the spectral characteristics could be qualitatively related to the height of the magma column and the corresponding style of volcanic activity (FALSAPERLA *et al.*, 1998; LANGER and FALSAPERLA, 2003). STEPHENS *et al.* (1994) developed a tool named SSAM devoted to the continuous monitoring of the spectral content of the seismic signals recorded on Redoubt volcano, Alaska. The Authors calculated spectra of sliding windows of the incoming signals, and represented the amplitudes of predefined frequency bins in spectrograms.

The analysis we propose is similar to the concept developed in the aforementioned SSAM, as we calculate spectrograms throughout the eruptive activity. At our reference station ETF (Fig. 1) the signal was little affected by high frequency attenuation due to its proximity to the eruptive centers; thus the frequency shifts turned out more evident than at the other stations. The spectrograms we depict in Figure 4 are calculated over a total time span of ca. 10 minutes, using a sliding window technique. The individual spectra, expressed in terms of power spectral density, are calculated applying a cosine bell window to time series of 2048 points, and performing the Fast Fourier Transform. The individual windows are shifted with a step width of 6 s, providing an overlap of about 50%. The parameters we choose for the calculation of the spectrograms allow us to reach a good compromise between the goal to show the development of spectra over significant time windows

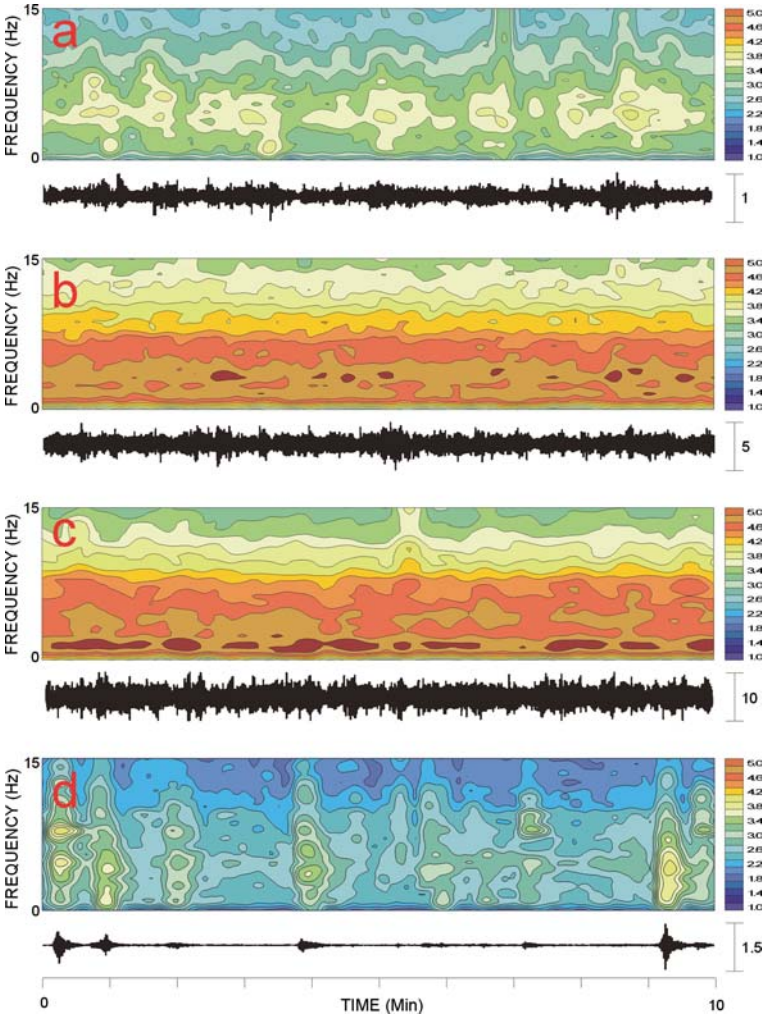

Figure 4
Spectrograms and corresponding seismograms at ETF. From top to bottom, the cartoons display the characteristics of the frequency content: a) before an episode of lava fountain preceding the effusive period (July 7, 2001), b) during a lava fountain (July 7, 2001), c) during the lava effusion (July 29, 2001), and d) after the flank eruption (September 7, 2001). The numbers close to the bars on the right of the seismograms allow scaling of the amplitude of the signal with respect to the pre-eruptive background depicted in a).

and to highlight features such as the presence of transients (e.g., tectonic earthquakes, explosion quakes) and/or fluctuations of the persistent tremor signal. It is worth noting that the identification of earthquakes is crucial for the separation of the source mechanisms associated with these signals from that of volcanic tremor. Indeed, transients with short duration such as earthquakes can significantly affect the frequency content of the signal. These frequency changes should not be

misunderstood as caused by the source of tremor, which is supposed to behave stationary, at least on a time scale of minutes or tens of minutes. Explosion quakes are recognizable as transients characterized by an upper frequency limit around 10 Hz, whereas tectonic earthquakes show dominant peaks also well above this limit.

In Figure 4a we depict a spectrogram of July 7, 2001, typical for the pre-effusive period. Besides the rather low overall amplitudes (light green and blue colors prevailing), we note dominant frequencies around 5 Hz. Isolated transients are present as well. For comparison with a paroxysm, we show the spectrogram representing the climax of the lava fountain which occurred the very same day (Fig. 4b). Unlike the spectrogram in Figure 4a, we find an enhanced overall amplitude level, with yellow, red, and brown colors distinctly dominant. Besides, there is a moderate frequency shift towards lower frequencies (ca. 3 Hz). Transient events are absent or, if there were, the tremor signal blotted them out, due to the high energy radiation. We observe a similar picture with enhanced overall tremor amplitude and dominant frequencies below 5 Hz in the days between July 9 and 11, 2001, i.e., about a week before the volcano unrest. During the lava effusion, the dominant spectral peaks markedly shifted towards even lower frequencies, reaching values of ca. 2 Hz from July 20 to 31, 2001 (Fig. 4c). In the weeks following the end of the flank eruption, the spectrograms of tremor showed small spectral amplitudes (blue colors prevailing), and dominant peaks around 5 Hz, whereas higher frequencies were associated with explosion quakes (Fig. 4d). Overall, the picture resembles the pre-effusive period shown in Figure 4a.

As aforementioned, the frequency shifts distinctly appeared at the station ETF. Nonetheless, they can also be recognized at the other stations. For example, at EMF and EMA the spectral maximum is between 2 Hz and 3 Hz at any time; however, the relative changes in the frequency content, towards lower or higher frequency values, vary with respect to the volcanic activity (Fig. 5). Accordingly, the signals at these stations have dominant frequencies closer to the lower bound (2 Hz) during the paroxysmal phases.

RMS Amplitude Ratios and Decay

We calculate the ratios of the signal amplitude between ETF and the five stations depicted in Figure 1 to investigate the spatial and temporal changes of the tremor source/s. For our analysis, we use the RMS amplitude values at each station, calculated over time spans of 30 s. For the calculation of each ratio in Figure 6, we first divide the RMS amplitude of the signal recorded at ETF for that of another station, and then apply a moving average of 15 min to highlight the overall trend. We exclude from our analysis the days between July 13 and 17, as the signal was severely affected by the occurrence of the VT swarm. Based on the development of the RMS

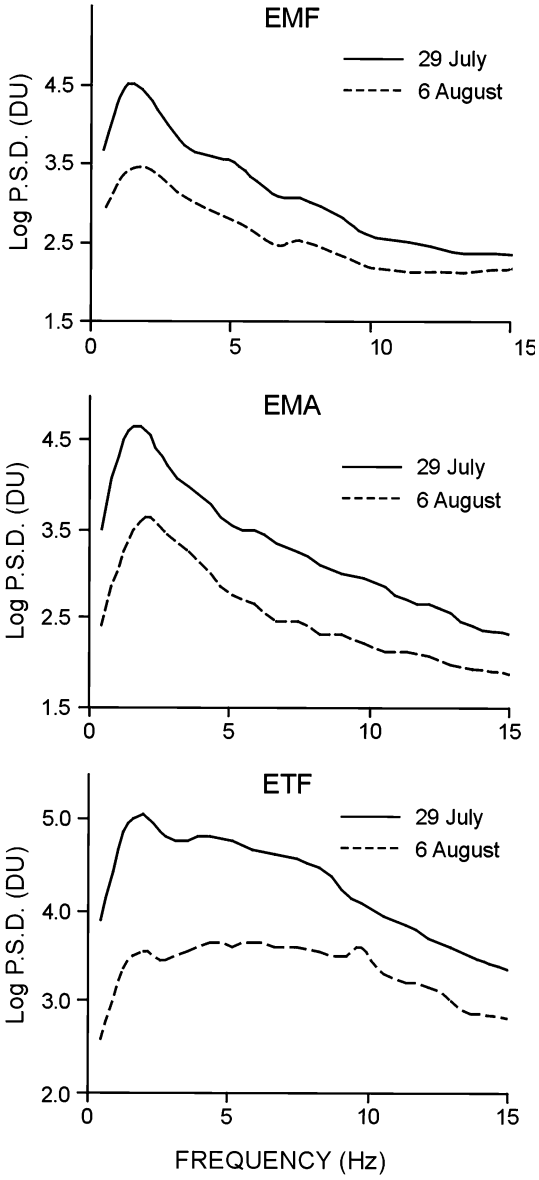

Figure 5
Power spectral density of velocity at the vertical component of the stations EMF, EMA, and ETF in two different days, i.e., on July 29 and August 6, 2001.

amplitude at ETF, which is depicted in Figure 3, we focus our analysis on four distinctive time windows (Figs. 6a–d). Each time window covers some 48 hours, and was chosen to describe: the pre-effusive phase (from July 10 to 12, Fig. 6a), the initial effusive phase characterized by increasing amplitude values (from July 19 to 20,

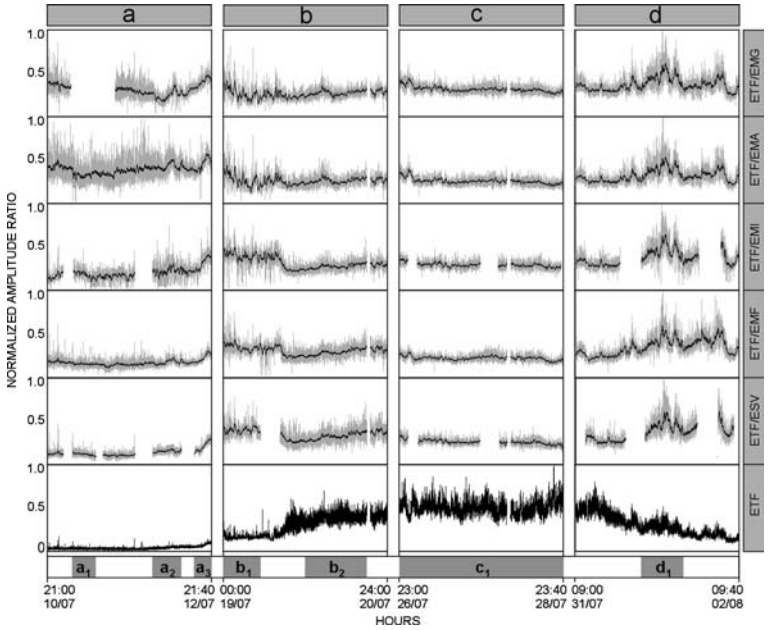

Figure 6

Normalized ratios of the RMS amplitude of the seismic signal at five couples of stations during four time windows: a) from July 10 at 21:00 to July 12 at 21:40, b) from July 19 at 00:00 to July 20 at 24:00, c) from July 26 at 23:00 to July 28 at 23:40, d) from July 31 at 09:00 to August 2 at 09:40. The couple of stations used for each ratio is indicated in the label on the right. Gray and black lines represent single values of the ratio and moving average over 15 min, respectively. The normalized RMS amplitude at the reference station ETF is depicted on the bottom. We label the time spans of signal in which we calculate the linear fit of the amplitude decay (see Fig. 7) with a_1, a_2 and a_3 in the pre-effusive phase, and b_1, b_2, c_1, d_1 in the effusive phase.

Fig. 6b), the phase of intense eruptive activity with high amplitudes of the seismic signal (from July 26 to 28, Fig. 6c), and the phase of decreasing amplitudes concurrent with the reduction of the effusion rate (from July 31 to August 2, Fig. 6d). At the bottom of Figure 6, we show the normalized RMS amplitude at ETF in the four time windows selected. We also normalize the amplitude ratios to the maximum value obtained for each couple of stations (upper five traces). In doing so, we can compare the relative variations throughout the aforementioned four phases.

July 10 – 12 (Fig. 6a)

The ratios ETF/EMF and ETF/ESV look very similar. The ratios for these couples of stations have small variations only, and the average values are almost steady. Conversely, the ratio ETF/EMA has considerable variability. Overall, in all the ratios the variability decreases in the final part of the time window analyzed. The

minor variability seems to be related to the enhancement in the signal amplitude which has been visible at ETF since the evening of July 12.

July 19 – 20 (Fig. 6b)

In the initial part of the cartoon there is a high variability of the single values (in gray in the figure) for all the ratios considered. The transition towards a lower variability is marked by a step-like decrease in the average values of the ratios ETF/EMI, ETF/EMF, and ETF/ESV.

July 26 – 28 (Fig. 6c)

This time span, which is characterized by the highest seismic energy radiation among the time windows selected, has the minor variability in the single values of the ratios with respect to the other phases. Overall, the values of the moving average look stationary for all the ratios.

July 31 – August 2 (Fig. 6d)

There is a great variability in the single values of all the ratios starting from the late morning of July 31. Unlike the previous time windows, we also observe remarkable changes even in the values of the moving average, which mark temporary outstanding rises in all the ratios.

Overall, we observe that the trends are similar for all the ratios during each phase, and are characterized by comparable changes in time. It is worth noting that the values of the ratios substantially varied concurrent with periods characterized by low tremor amplitudes, e.g., first phase, initial part of the second phase, and final part of the fourth one (Figs. 6a–b, d). Conversely, in a period of high intensity of the flank eruption (third phase), the ratios had fairly stationary values (Fig. 6c). Eventually, during the final part of the lava emission, we notice enhanced values of the amplitude ratios which support the hypothesis of an increased energy radiation at ETF with respect to the other stations (fourth phase). Here the picture is complicated by the presence of frequent transients (explosion quakes), which mostly affected the calculation of the RMS amplitudes at ETF (Fig. 6d).

Based on the decay of the amplitude at our stations, we also look for the location of the source of volcanic tremor. We refer our analysis to time windows marked with a_1, a_2, and a_3 in Figure 6a (pre-effusive phase), and b_1, b_2, c_1, and d_1 in Figures 6b–d (effusive phase). For this analysis, we assume an isotropic radiation of the seismic waves, and a source region whose initial position is located: i) below the summit craters, or ii) in the middle of the eruptive field (Fig. 1). With the latter assumption we initially attribute most of the contribution of seismic energy: i) to the main volcanic feeder, which was one of the ''engines'' of the lava emission, ii) to the dike. Accordingly, we first project the position of the source on the topographic surface, and calculate the logarithm of the station-to-source distances. Then, using the logarithm of the RMS

amplitude at each station, we apply a linear fit to these values, considering different depths of the source starting from 0 to 12 km, at intervals of 500 m. For the sake of readability, we depict the results obtained with steps of 1 km for depths ranging from 0 to 6 km in Figure 7a (pre-effusive phase), and with steps of 500 m for depths ranging from 0 to 3 km in Figure 7b (effusive phase), assuming a position of the source below the summit craters. This assumption is indeed the one which gives us the best results. We exclude EMI and EMG from Figure 7, as before the convulsive days following the onset of the flank eruption there was an unknown change in the amplification of these stations for which we cannot correct the amplitude of the signal. Moving from the left to the right-hand column in Figure 7a, we observe that the best fits in the pre-effusive phase are linked to a position of the source which becomes shallower and shallower. Based on the goodness of the fits (R^2), we infer the depth of the source from the highest R^2 value for each curve depicted in Figure 8. Accordingly, we find depths of 5 km (a_1), 3.5 km (a_2), and 1 km (a_3) with a range of approximation constrained by the step of 0.5 km of our analyses (Fig. 8). Throughout the effusive phase, we observe that the best fits are all linked to a superficial position (within 500 m from the surface) of the source (Fig. 7b). As the results for the time windows marked as b_1 and b_2 are very similar (see Fig. 8), we exhibit in Figure 7b only those concerning b_1. The goodness of the fits for the amplitude decay during the period from 26 July at 23:00 to 28 July at 23:40 (Fig. 7b, central column) is generally better than that in the other time spans of the effusive phase (see also c_1 in Fig. 8). Reasonably, we can assess that, according to the amplitude decay, the results obtained for the whole effusive phase (Fig. 7b) are in favor of a source closer to ETF than the other stations. Additionally, we believe that this finding cannot be attributed to a specific source, for it is the combined effect of different, even though inseparable, sources acting at the same time.

Tremor and Volcanic Activity during the July – August 2001 Flank Eruption

In Figure 9 we portray the RMS amplitude of the signal at ETF after applying a moving average over 5 hours. The total time span represented in Figure 9 ranges from two weeks before to four days after the flank eruption. Small gaps are filled using a linear interpolation between adjacent values. The content of the figure is

▶

Figure 7

RMS amplitude of the seismic signal versus the station-to-source distance during: a) the pre-effusive phase, and b) the effusive phase. In a) the windows from the left to the right-hand column correspond to the time spans marked as a_1, a_2 and a_3 in Figure 6a. In b) the windows in the left-hand column refer to the time span marked as b_1 in Figure 6b; the windows in the central column refer to c_1 in Figure 6c, and those in the right-hand column refer to d_1 in Figure 6d. All values are in logarithmic scale. The distances from the source are depicted in a) in a range of depth from 0 to 6 km, with step of 1 km, and in b) from 0 to 3 km, with step of 500 m. The RMS amplitudes in the vertical bars refer to the stations: ETF (A), ESV (B), EMF (C), and EMA (D). The equation of the linear fit (dashed line) is indicated on the top right of each window along with the value of R^2.

comparable with the information reported in Figure 3. Nevertheless, the longer moving average allows us to display the data in a time window which is more convenient to highlight the temporal relationships between changes in the RMS amplitude and style of volcanic activity. Detailed reports treating the on-going flank

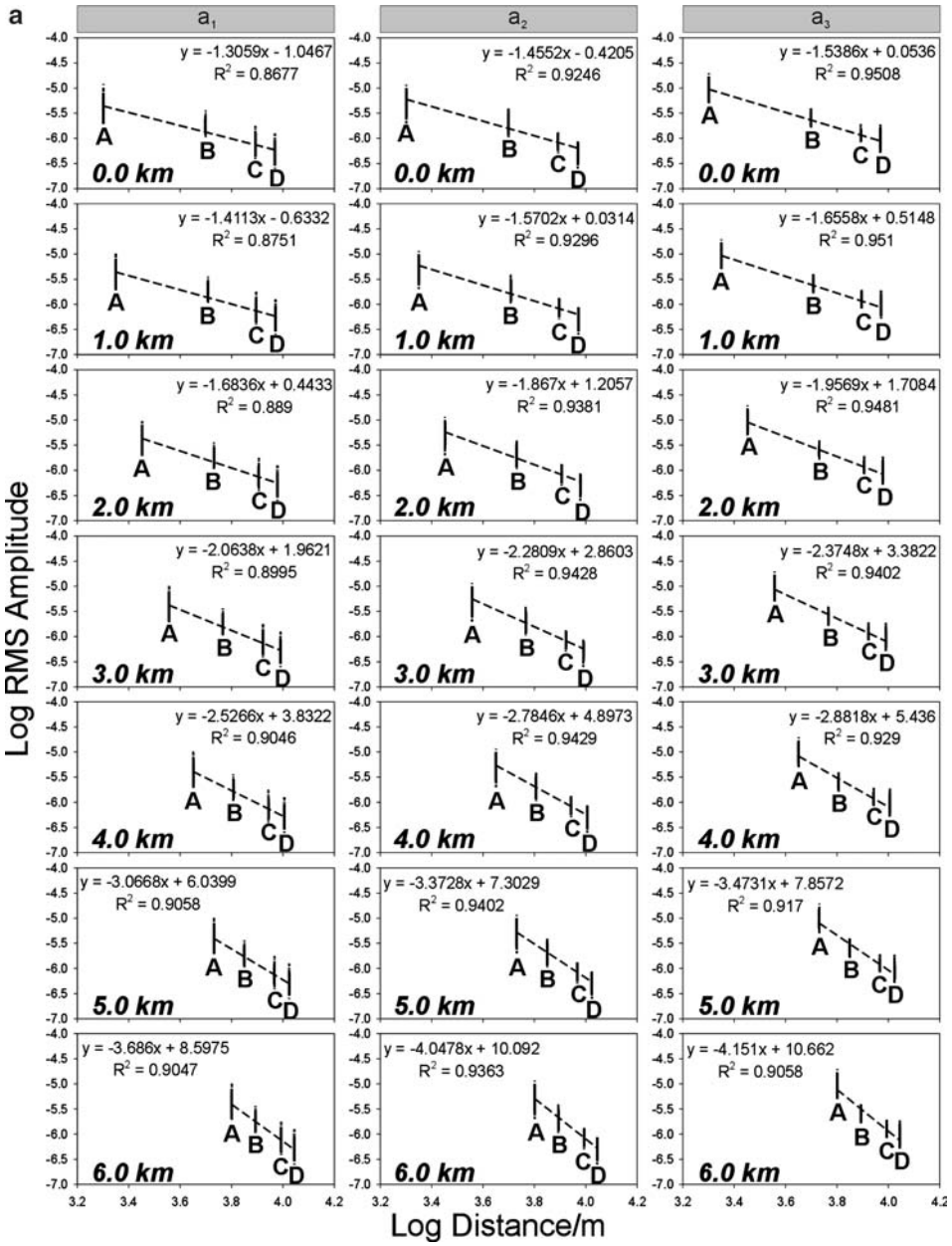

eruption were provided by volcanologists of INGV, who daily surveyed the eruptive field (Research staff of INGV, 2001). Accurate reconstructions of the eruptive style

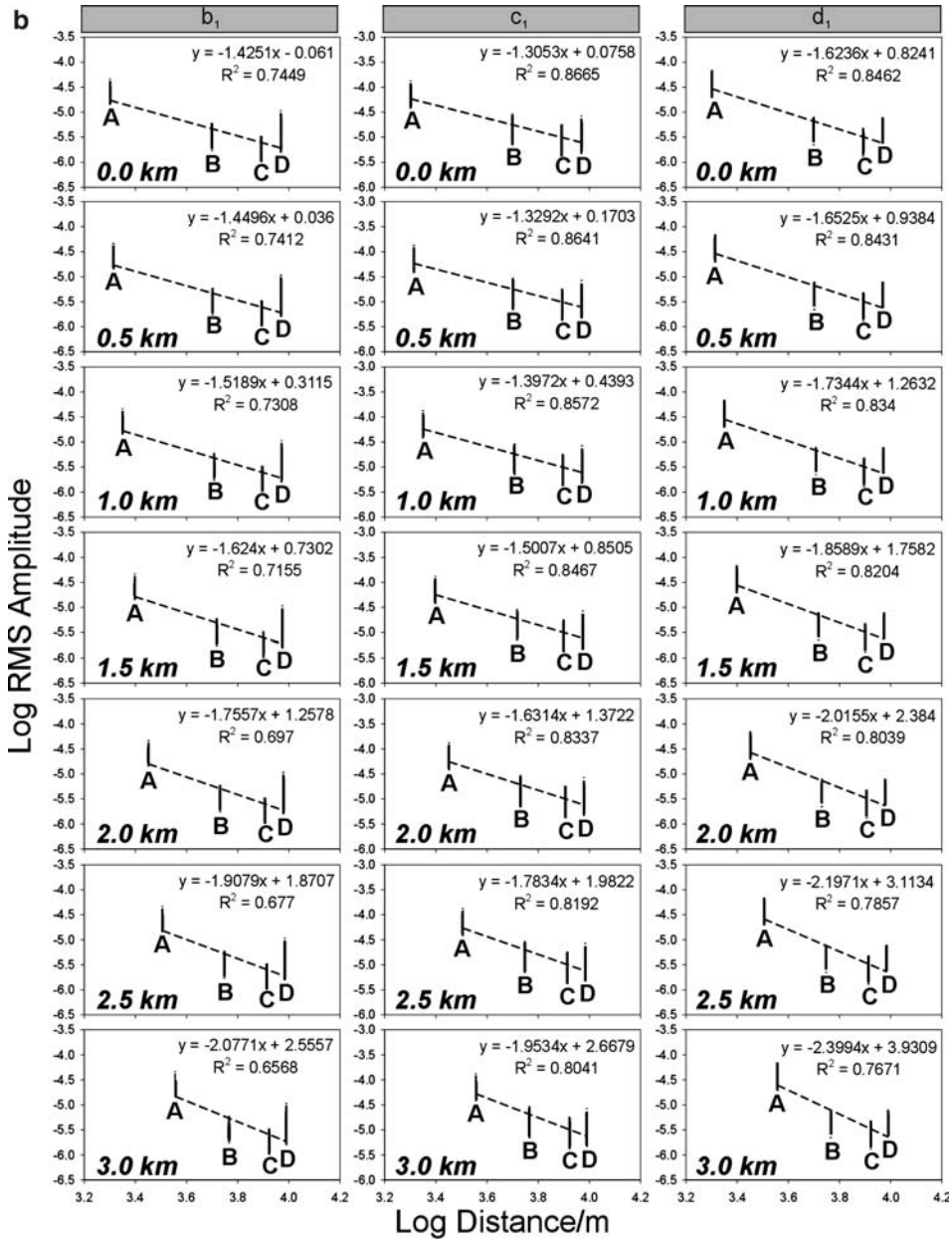

Figure 7
(Contd.)

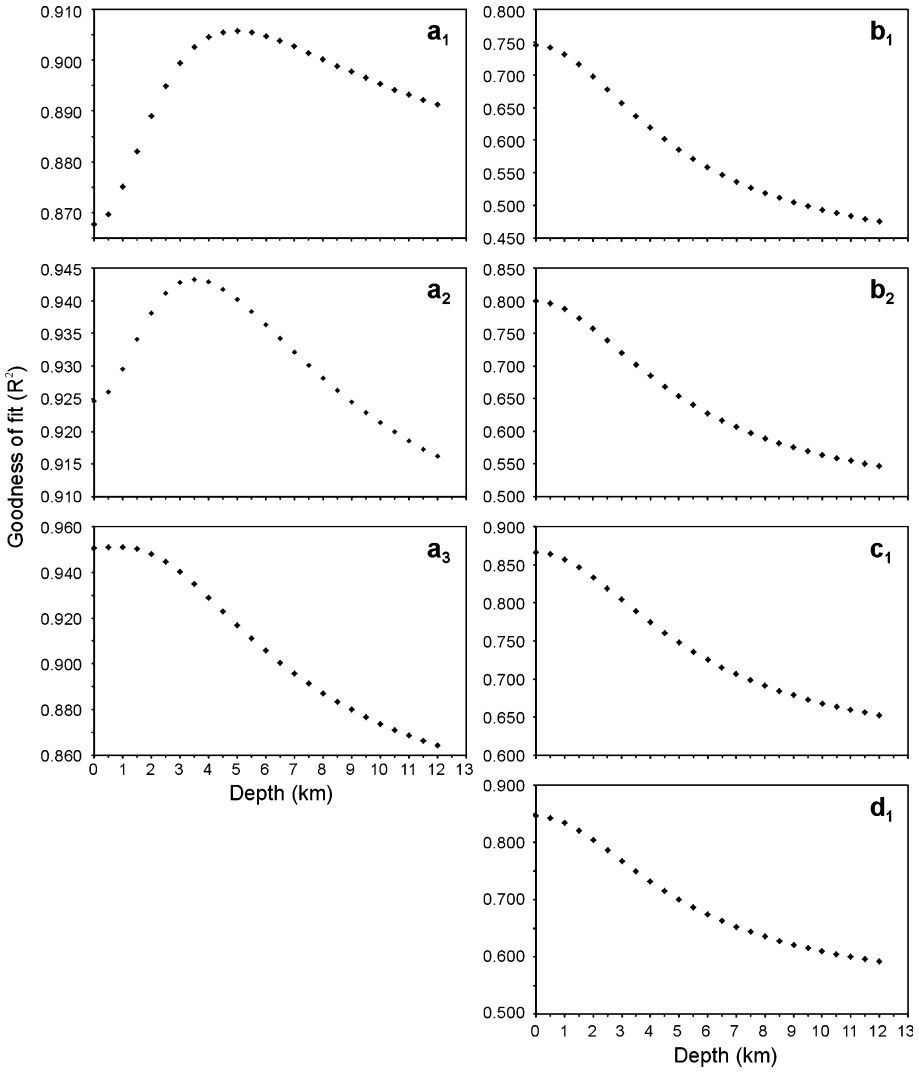

Figure 8
Goodness of the fit (R^2) versus depth. The values of R^2 refer to the linear fit calculated for the decay of the amplitude at the stations ETF, ESV, EMF, and EMA at depths from 0 to 12 km, with step of 500 m. The labels a_1, a_2, a_3, b_1, b_2, c_1, d_1 refer to the time windows marked at the bottom of Figure 6 in which we calculate the amplitude decay.

have been subsequently published (e.g., BEHNCKE and NERI, 2003; LANZAFAME *et al.*, 2003). Accordingly, we analyze the temporal changes of the RMS amplitude and relate them to the activity reported at the main eruptive centers, i.e., the summit area, and the two peripheral vents at 2550 m and 2100 m asl, respectively. Based on the aforementioned observations of volcanic activity, we distinguish three main

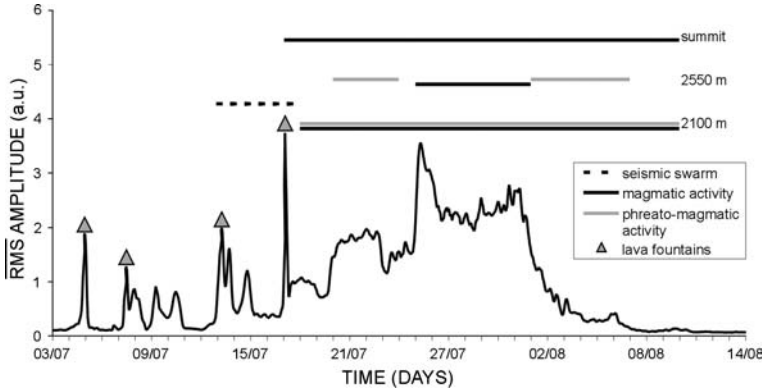

Figure 9
Moving average over 5 hours of the RMS amplitude recorded at ETF between 00:00 of July 3 and 00:00 of August 14, 2001. Gray and black lines on top of the cartoon mark the different styles of volcanic activity at the three main eruptive centers. Gray triangles and dashed line indicate the occurrence of lava fountain episodes and seismic swarm, respectively.

stages in the tremor amplitude associated with variations in seismic energy radiation (Fig. 9).

The first stage was characterized by a saw teeth trend due to the repeated occurrence of lava fountains in the time span between July 3 and 17 (Fig. 9). Particularly from July 3 to 12, the RMS amplitude alternated between moments of low energy radiation and episodes of lava fountains which show up as sharp peaks in Figure 9. From July 12 to 17, tremor amplitudes in between the new episodes of lava fountains did not return to the former background values, remaining on levels at least twice as high as recorded at the beginning of the month. The swarm of tectonic events further enhanced the RMS amplitude. By July 17, concurrent with the VT swarm, a strong episode of lava fountaining heralded the onset of the volcano unrest. The same day we observed the highest peak in Figure 9, which marked the onset of lava effusion as well.

The second stage started on July 18 and finished on July 31 (Fig. 9). After the conclusion of the episode of lava fountain on July 17 and the subsequent drop of the RMS amplitude, the seismic energy radiation returned to increase remarkably throughout the flank eruption. The beginning of phreatomagmatic activity at the peripheral vent at 2550 m on July 19 was accompanied by a sudden increase in the tremor amplitude. A further abrupt increase occurred between July 24 and 25, concurrent with the change in the eruptive style at this vent from phreatomagmatic to magmatic. Although with some fluctuation, the RMS amplitude remained high until the morning of July 31. The third stage started during the same day of July 31, when at the eruptive vent at 2550 m magmatic activity ended and phreatomagmatic activity resumed (Fig. 9). The RMS amplitude concurrently marked a dramatic

decrease in the energy radiation, which continued unrelentingly in the following days. From August 1 onward, the volcanic activity at the summit and at the eruptive vents at 2100 m became weaker and weaker, until the lava emission stopped completely on August 9. Nevertheless, even small, brief enhancements in the visible volcanic activity were clearly associated with temporary changes in the development of the RMS amplitude, despite its overall decreasing trend. The RMS amplitude reached its pre-effusive background level on August 9, when all visible volcanic activity died out (Fig. 9).

Discussion

Mt. Etna's unrest on July 17, 2001 marks the climax of an evolution of the volcanic system lasting several years (PATANÈ *et al.*, 2003b). From the conclusion of the flank eruption of December 1991 – March 1993 onward, summit activity yielded a variety of eruptive episodes mostly in forms of powerful Strombolian explosions, lava fountains, and overflows. Episodes of lave fountains with origins from the Southeast and Northeast craters deserved particular attention (e.g., ALPARONE *et al.*, 2003). The repetitive character of these lave fountains – fifteen of which occurred in 2001 (Table 1) – may be reasonably explained assuming: i) a storage of a good deal of magma at a relatively shallow depth, and ii) an efficient replenishment of the feeder, which assures the continuity of the eruptive activity over years. Petrological analysis of the products erupted between 1995 and 1999 strongly supports this explanation, highlighting processes of superficial storage, cooling, and crystallization of magma (CORSARO and POMPILIO, 2004). Such processes diversely affected the composition of the products of the active craters, according to the variable magma upwelling from depth. The analysis of gravimetric data spatially constrained the storage of a large volume of magma at 2 km bsl (CARBONE *et al.*, 2003a, b), in good agreement with ground deformation data based on EDM and GPS measurements, which highlighted an increasing average areal dilatation from 1994 on (BONACCORSO *et al.*, 2002). The resumption of VT seismicity during Fall 1994 and the foci location until the unrest of July 17, 2001 were further evidence of a dike intrusion, at a depth of between 2 and 5 km bsl (PATANÈ *et al.*, 2002, 2003a). The location of the dike was well constrained by seismic tomography at ca. 1–2 km bsl, 300–500 m east of the fracture system (PATANÈ *et al.*, 2002). Geochemical evidence from periodic COSPEC and FTIR measurements led to postulation of an increasing storage of magma from 1994 forward, which was inferred from the ratio between the estimated input from depth and the quantity of magma emitted during the eruptive episodes preceding the impending eruption (CALTABIANO *et al.*, 2004).

The analysis of tremor at Mt. Etna has yielded valuable information on the long-term (e.g., from months to years) as well as short-term (days to weeks) changes in the volcanic system (e.g., COSENTINO *et al.*, 1989; CARDACI *et al.*, 1993; ALPARONE

et al., 2003). In many volcanoes worldwide tremor is recorded in the form of storms, such as those reported during phases of lava-dome building at Merapi (SEIDL *et al.*, 1990), or swarms of long-period and/or hybrid events which merge into sustained tremor, as happened at Redoubt (CHOUET *et al.*, 1994) and Monserrat (NEUBERG *et al.*, 1998). Unlike these volcanic areas, tremor is continuously present at Mt. Etna, albeit changing in amplitude and frequency content. The persistent presence of tremor discloses the possibility to analyze the relationships which link this signal to volcanic activity. For example, episodes of lava fountains, recorded at the permanent video camera of INGV, pointing to the summit craters, have a strict link to the increase in the amplitude of the seismic signal (ALPARONE *et al.*, 2003; PATANÈ *et al.*, 2004). This close relationship was fundamental for forecasting the paroxysms which occurred in 2001 (Table 1), and allowed the INGV's staff to alert the Civil Defense and the air traffic authorities of the international airport of Catania Fontanarossa for the hazard of ash clouds and fallout. We note that the spectral features of tremor during lava fountains highlight a remarkable decrease in the dominant frequencies with respect to the background signal (Figs. 4a–b). The increase in amplitude marks another striking change in the signal, for it can be recorded at seismic stations as far as tens of kilometers from the craters. Particularly, we observe that the high seismic energy radiation recorded during the July – August, 2001 flank eruption shares features which are similar to those highlighted in the aforementioned episodes of lava fountains (Figs. 4b–c). On the other hand, we observe strong differences in the frequency content, in terms of presence of the dominant (i.e., largest) peaks in an even lower frequency bound than throughout a lava fountain (Figs. 4b–c). This effect is particularly evident at ETF, which usually has higher frequency content than the other stations (Fig. 5). We surmise that the closeness to the active craters and eruptive fissures makes the signal at ETF less affected by attenuation.

We interpret the overall picture derived from Figures 4, 6, 7 and 9 in terms of increasing/decreasing activation of various sources. In pre-effusive time, the background seismic energy radiation highlighted temporary enhancements due to lava fountains. In our opinion, the episodes of lava fountains and powerful Strombolian activity of Table 1 were due to the activation of a source which intersected the conduits of the main feeder. The repetitiveness of the paroxysms before the July – August, 2001 flank eruption supports the hypothesis of a reservoir whose activation was regulated by conditions of pressurization, similar to a geyser (e.g., KIEFFER, 1984). Based on the amplitude decay of the signal, we surmise that a dike migrated from about 5 km to ca. 1 km in the time span from July 10 at 21:00 and July 12 at 21:40. We postulate that during the night of July 17 the high amplitude of tremor (Fig. 9) was caused by the concurrent activation of three different volcanic sources, i.e., the peripheral dike which fed the eruption, the reservoir which fed the lava fountains, and the central conduit. After the unrest, the energy of the seismic signal concealed the contributions of the single sources. During the flank eruption we note: (i) sustained high tremor radiation (Figs. 3, 9) over the whole volcano unrest,

(ii) a shift of the dominant spectral content towards frequencies lower than the pre-effusive period (Fig. 4), (iii) an increasing area affected by strong seismic radiation, which encompassed sites from ETF to more distant stations (see Fig. 6). By July 31, we observed a general decrease in tremor amplitude, which was more pronounced at the more distant stations. This is evident in Figure 6d where the amplitude ratios tend to be higher in the presence of transients to which ETF is more sensitive. It is worth mentioning that a combined use of seismic, acoustic and thermal sensors was carried out close to the active vent at 2550 m from August 3 to the end of the flank eruption. Based on these comparative measurements, GRESTA *et al*. (2004) estimated the depth of the seismic source at the origin of explosive activity at about 250 m below the pre-existing ground surface.

Exploiting common concepts of classical earthquake seismology, we may postulate a relation between the size of the area with strong seismic signals and the depth of the source. Our analysis of the amplitude decay (Fig. 7) and the changes in the goodness of the fits (Fig. 8) highlight that the dike moved fast, from about 5 km to the surface starting from July 10. Additionally, we find that the position of the source was shallow (within 500 m) and closer to ETF than the other stations shortly after the onset of the lava effusion, in a phase of intense effusive activity as well as towards the final stage of the flank eruption (see Figs. 6b–d, Fig. 7b, and Fig. 8). Actually, given our network geometry and the limited number of stations, we cannot locate the dike separately throughout the lava effusion, as the lateral extension of the dike makes it indistinguishable from the main volcanic feeder.

The relationship between volcanic activity and development of tremor in time offers a powerful tool for exploring the eruptive style and the mechanisms which control it. This relationship was particularly evident at the active center at an elevation of 2550 m. From July 20 on, phreatomagmatic activity was concurrent with a phase of rapid tremor amplitude increase. The highest peak of tremor amplitude marked a change in the eruptive style from phreatomagmatic to magmatic, concurrent with an enhanced magma effusion rate reported by BEHNCKE and NERI (2003). By July 31, tremor amplitudes decreased rapidly, marking again a change in the eruptive style from magmatic to phreatomagmatic before the activity of this volcanic center died out on August 3. The increase of RMS amplitude in the seismic signal during episodes of lava fountains, as well as the changes observed at the transition from phreatomagmatic to magmatic activity and *vice versa* (Fig. 9) have proved to be extremely useful for the alert of civil authorities. Additionally, update information on volcanic tremor became of fundamental importance in the event of bad weather and when the conditions of the eruptive field made it inaccessible at or unsafe for direct survey.

Conclusions

The continuous tremor recorded on Mt. Etna allows us to investigate the changes in this signal before, at the onset, and during the July – August 2001 flank eruption. We find that the frequency content of tremor decreases from pre-effusive to effusive stages. Additionally, different values of the frequency content are associated with diverse styles of eruptive activity (e.g., lava fountains, phreatomagmatic activity, Strombolian explosions, lava emission), changing from the usual 5 Hz at our reference station ETF close to the summit craters of the volcano, to about 3 Hz during episodes of lava fountains, or to about 2 Hz during phases of intense lava emission.

Based on the amplitude decay of the signal at our stations, we find that: i) the position of the dike migrated from about 5 km to ca. 1 km from July 10 to July 12; ii) the source of tremor was within 500 m from the surface on July 19, i.e., shortly after the onset of the flank eruption, and was closer to ETF than the other seismic stations until July 31 – August 2, when the lava emission was about to cease.

Overall, we conclude that it is possible to follow the complete time-history of the 2001 flank eruption on the basis of tremor data analysis. In a multidisciplinary perspective, our approach is a contribution to the mass of data which can be recorded at Mt. Etna. Tremor analysis has shown to be effective, and can be extremely useful in this as in other volcanic areas where remote control of tremor may temporary become or is usually the only possible, and safe, way to survey volcanic activity.

Acknowledgements

We are indeed grateful to two anonymous reviewers for their useful comments and suggestions which helped us to significantly improve the quality of the paper. We express our gratitude to Dr. Shimazaki for his encouragements throughout the preparation of the revised version of the manuscript. Finally, we thank Alfio Amantia for kindly providing the picture of Mt. Etna in Fig. 2. This work was financially supported by the Gruppo Nazionale per la Vulcanologia, Italy.

References

Alparone, S., Andronico, D., Lodato, L., and Sgroi, T. (2003), *Relationship between Tremor and Volcanic Activity during the Southeastern Crater Eruption on Mount Etna in Early 2000,* J. Geophys. Res. *108* (B5), 2241, doi:10.1029/2002JB001866.

Armienti, P., Pareschi, M.T., Innocenti, F., and Pompilio, M. (1994), *Effects of Magma Storage and Ascent on the Kinetics of Crystal Growth. The Case of the 1991–93 Mount Etna Eruption,* Contrib. Mineral. Petrol. *115*, 402–414.

BARBERI, F., CARAPEZZA, M.L., VALENZA, M., and VILLARI, L. (1993), *The Control of Lava Flow during 1991–1992 Eruption of Mount Etna,* J. Volcanol. Geotherm. Res. *56*, 1–34.

BEHNCKE, B. and NERI, M. (2003), *The July – August 2001 eruption of Mt. Etna (Sicily)*, Bull. Volcanol. *65*, 461–476.

BONACCORSO, A., ALOISI, M., and MATTIA, M. (2002), *Dike Emplacement Forerunning the Etna July 2001 Eruption Modelled through Continuous Tilt and GPS Data*, Geophys. Res. Lett. *29* (13), 10.1029/2001GL014397.

CALTABIANO, T., BURTON, M., GIAMMANCO, S., ALLARD, P., BRUNO, N., MURÈ, F., and ROMANO, R. (2004), *Volcanic gas emissions from the summit craters and flanks of Mt. Etna, 1987–2000*. In *Mt. Etna: Volcano Laboratory*, AGU Monograph 143 (eds. A. Bonaccorso, S. Calvari, M. Coltelli, C. Del Negro, and S. Falsaperla), pp. 111–128.

CALVARI, S., COLTELLI, M., POMPILIO, M., and NERI, M. (1994), *1991-1993 Etna Eruption: Geological Observation and Chronology of Eruptive Events*, Acta Vulcanol. *4*, 1–14.

CARBONE, D., BUDETTA, G., and GRECO, F. (2003a), *Possible Mechanisms of Magma Redistribution under Mt. Etna during the 1994–1999 Period Detected through Microgravity Measurements*, Geophys. J. Int. *152*, 1–14.

CARBONE, D., BUDETTA, G., and GRECO, F. (2003b), *Bulk Processes prior to the 2001 Mount Etna Eruption, Highlighted through Microgravity Studies*, J. Geophys. Res. *108* (B12), 2556, doi: 10.1029/2003JB002542.

CARDACI, C., FALSAPERLA, S., GASPERINI, P., LOMBARDO, G., MARZOCCHI, W., and MULARGIA, F. (1993), *Cross-correlation Analysis of Seismic and Volcanic Data at Mt. Etna Volcano*, Italy. Bull. Volcanol. *55*, 596–603.

CHOUET, B.A., PAGE, R.A., STEPHENS, C.D., LAHR, J.C., and POWELL, J.A. (1994), *Precursory Swarms of Long-period Events at Redoubt Volcano (1989–1990), Alaska: Their Origin and Use as a Forecasting Tool*, J. Volcanol. Geotherm. Res. *62*, 95–136.

CORSARO, R.A. and POMPILIO, M. (2004), *Magmatic Processes in Magma Dynamics the Shallow Plumbing System of Mt.Etna as Recorded by Compositional Variations in Volcanics of Recent Summit Activity (1995–1999)*, J. Volcanol. Geotherm. Res., *137*, 55–71.

COSENTINO, M., LOMBARDO, G., and PRIVITERA, E. (1989), *A Model for Internal Dynamical Processes on Mt. Etna,* Geophys. J. *97* (3), 367–379.

FALSAPERLA, S., LANGER, H., and SPAMPINATO, S. (1998), *Statistical Analysis and Characteristics of Volcanic Tremor on Stromboli volcano (Italy),* Bull. Volcanol. *60*, 75–88

FALSAPERLA, S., PRIVITERA, E., CHOUET, B., and DAWSON, P. (2002), *Analysis of Long-period Events Recorded on Mt. Etna (Italy) in 1992, and their Relationship with Eruptive Activity*, J. Volcanol. Geoth. Res. *114* (3–4), 421–442.

FALSAPERLA, S., PRIVITERA, E., SPAMPINATO, S., and CARDACI, C. (1994), *Seismic Activity Related to the December 14, 1991 Mount Etna Eruption*, Acta Vulcanol. *4*, 63–73.

GORDEEV, E.I., SALTYKOV, V.A., SINITSYN, V.I., and CHEBROV, V.N. (1990), *Temporal and Spatial Characteristics of Volcanic Tremor Wavefields*, J. Volcanol. Geotherm. Res. *40*, 89–101.

GRESTA, S., RIPEPE, M., MARCHETTI, E., D'AMICO, S., COLTELLI, M., HARRIS, A.J.L., and PRIVITERA, E. (2004), *Seismoacoustic Measurements during the July-August 2001 Eruption of Mt. Etna Volcano, Italy*, *137*, 219–230. J. Volcanol. Geotherm. Res.

LANGER, H., and FALSAPERLA, S. (2003), *Seismic Monitoring at Stromboli Volcano (Italy): A Case Study for Data Reduction and Parameter Extraction*, J. Volcanol. Geoth. Res. *128*, 233–245.

LANZAFAME, G., NERI, M., ACOCELLA, V., BILLI, A., FUNICELLO, R., and GIORDANO, G. (2003), *Structural Features of the July–August 2001 Mount Etna Eruption: Evidence for a Complex Magma Supply System*, J. Geol. Soc. London *160*, 531–544.

KIEFFER, S. (1984), *Seismicity at Old Faithful Geyser: An Isolated Source of Geothermal Noise and Possible Analogue of Volcanic Seismicity,* J. Volcanol. Geotherm. Res. *22*, 59–95.

NEUBERG, J., BAPTIE, B., and LUCKETT, R. (1998), *Results from the Broadband Seismic Network on Montserrat*, Geophys. Res. Lett. *25* (19), 3661–3664.

PATANÈ, D., CHIARABBA, C., COCINA, O., and DE GORI, P. (2002), *Tomographic Images and 3D Earthquake Locations of the Seismic Swarm Preceding the 2001 Mt. Etna Eruption: Evidence for a Dyke Intrusion*, Geophys. Res. Lett. *29* (10), 10.1029/2001GL014391.

PATANÈ, D., COCINA, O., FALSAPERLA, S., PRIVITERA, E., and SPAMPINATO, S. (2004), *Mt. Etna volcano: A seismological framework*. In *Mt. Etna: Volcano Laboratory*, AGU Monograph 143 (eds. A. Bonaccorso, S. Calvari, M. Coltelli, C. Del Negro, and S. Falsaperla) pp. 147–165.

PATANÈ, D., DE GORI, P., CHIARABBA, C., and BONACCORSO, A. (2003b), *Magma Ascent and the Pressurization of Mount Etna's Volcanic System*, Science *299*, 2061–2063.

PATANÈ, D., PRIVITERA, E., GRESTA, S., AKINCI, A., ALPARONE, S., BARBERI, G., CHIARALUCE, L., COCINA, O., D'AMICO, S., DE GORI, P., DI GRAZIA, G., FALSAPERLA, S., FERRARI, F., GAMBINO, S., GIAMPICCOLO, E., LANGER, H., MAIOLINO, E., MORETTI, M., MOSTACCIO, A., MUSUMECI, C., PICCININI, D., REITANO, D., SCARFÌ, L., SPAMPINATO, S., URSINO, A., and ZUCCARELLO, L. (2003a), *Seismological Features and Kinematic Constraints for the July–August 2001 Lateral Eruption at Mt. Etna Volcano, Italy*, Annals of Geophys. *46* (4), 599–608.

RESEARCH STAFF OF INGV, Sez. di Catania (2001), *Multidisciplinary Approach Yields Insight into Mt. Etna Eruption*, EOS, Trans. AGU *82* (52), 653, 656.

SCHICK, R., COSENTINO, M., LOMBARDO, G., and PATANÈ, G. (1982), *Volcanic Tremor at Mount Etna – A Brief Description*. In *Mount Etna Volcano*. Mem. Soc. Geol. It. *23*, 191–196.

SCHICK, R. and RIUSCETTI, M. (1973), *An Analysis of Volcanic Tremors at South Italian Volcanoes*, Zeitshr. Geophys. *39*, 247–262.

SEIDL, D., KIRBANI, S.B., and BRÜSTLE, W. (1990), *Maximum Entropy Spectral Analysis of Volcanic Tremor Using Data from Etna (Sicily) and Merapi (Central Java)*, Bull. Volcanol. *52*, 460–474.

SEIDL, D., SCHICK, R., and RIUSCETTI, M. (1981), *Volcanic Tremors at Etna: A Model for Hydraulic Origin*, Bull. Volcanol. *44*, 43–56.

STEPHENS, C.D., CHOUET, B.A., PAGE, R.A., LAHR, J.C., and POWER, J.A. (1994), *Seismological Aspects of the 1989–1990 Eruptions at Redoubt Volcano, Alaska: The SSAM Perspective*, J. Volcanol. Geotherm. Res. *62*, 153–182.

(Received February 2, 2004; accepted November 18, 2004)
Published Online First: July 29, 2005